

## Chapter 7

# Ensemble variational methods

In this chapter, we look into the many ways to combine the benefits of variational and ensemble Kalman methods. The focus will mainly be on these developments in the domain of numerical weather prediction (NWP). We believe, however, that their applicability is much broader.

Combining the advantages of both classes of methods, one also wishes to avoid their drawbacks. From a theoretical standpoint, the EnKF propagates the error estimates and has a dynamical, flow-dependent representation of them. It also does not require the tangent linear and adjoint models of the observation operator, as seen from (6.11) of Chapter 6. On the other hand, 4D-Var by definition operates on a DA time window over which asynchronous observations can consistently, i.e., modelwise, be assimilated. Moreover, 4D-Var can perform a full nonlinear analysis within its DA window (abbreviated DAW in this chapter) thanks to numerical optimization techniques. On the downside, the EnKF requires the use of regularization techniques, inflation and localization, to filter out sampling errors and address the rank deficiency issue of the ensemble. 4D-Var requires the use of the tangent linear and adjoint models (evolution and observation), which are very time-consuming to derive and maintain. Other advantages and drawbacks, some of them pertaining to the practical implementation of the methods in high-dimensional NWP systems, are documented in Lorenc [2003] and Kalnay et al. [2007].

The investigations of NWP centers on the performance of both classes of methods have not shown very significant differences for synoptical meteorology. Indeed, the current operational DA systems for synoptic scale meteorology are rather Gaussian because of the dense and frequent observations of the atmosphere. Hence, it may be expected that well-tuned EnKF and 4D-Var should perform similarly in this context. However, this does not hold in general and in particular for significantly non-Gaussian DA systems.

The performance of the EnKF and 4D-Var can be compared on the Lorenz-95 model (see Section 6.7.3.1) in various regimes of nonlinearity. For instance, Figure 7.1 compares the performance of the EnKF (and the smoother EnKS described in Section 6.8) with 4D-Var as a function of the length of the DAW. For short windows, the EnKF and EnKS outperform 4D-Var because they both propagate the error statistics between two analyses using the perturbations simulated by the ensemble, whereas 4D-Var only propagates a mean state estimator. For longer DAWs, 4D-Var outperforms the EnKF

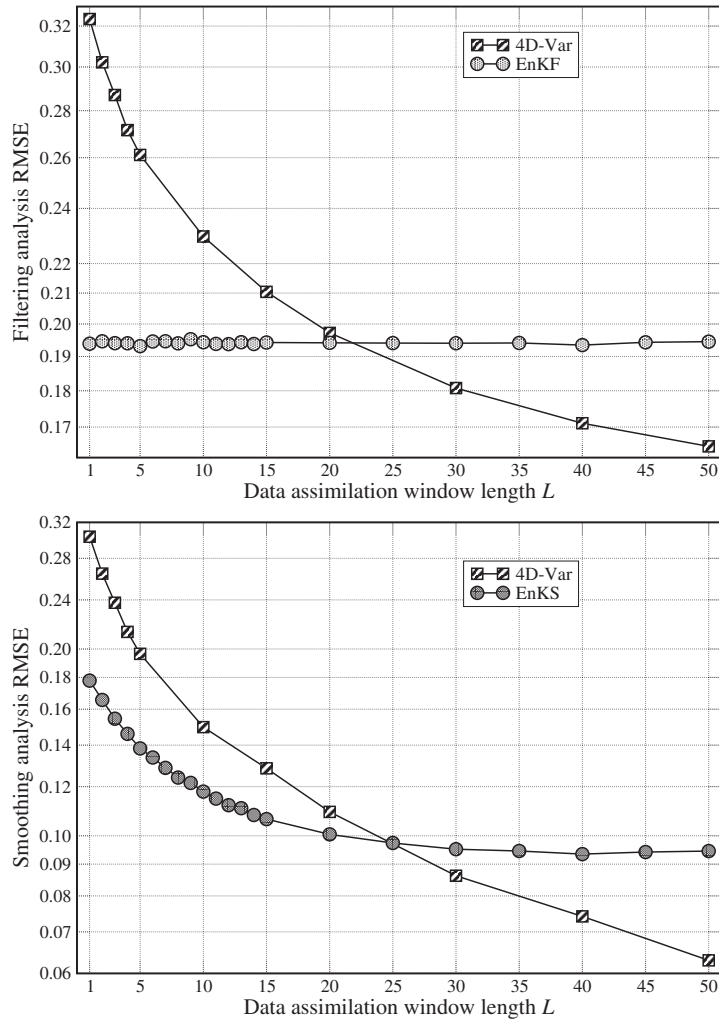


**Figure 7.1.** Synthetic DA experiments with the Lorenz-95 model, which emphasizes the distinct performance of the EnKF and 4D-Var. The upper panel shows the filtering analysis RMSE of optimally tuned EnKF and 4D-Var DA experiments as a function of the length of the 4D-Var DAW. The lower panel shows the smoothing analysis RMSE of optimally tuned EnKS and 4D-Var as a function of the length of their DAW. The optimal RMSE is chosen within the window for 4D-Var. The EnKF and the EnKS use an ensemble of  $m = 20$ , which avoids the need for localization but requires inflation. The length of the DAW is  $L \times \Delta t$ , where  $\Delta t = 0.05$ .

and the EnKS because of its full nonlinear analysis within the DAW. Hence, there must be room for an improved approach by properly combining the two methods—see Figure 1.5.

In this chapter, we will discuss four main classes of emerging systems that combine ensemble and variational methods. All these methods can generically be called *ensemble variational* or *EnVar* methods, as recommended by A.C. Lorenc and a WMO THORPEX working group.<sup>32</sup> These methods share ideas, principles, and many

<sup>32</sup>[http://www.wcrp-climate.org/WGNE/BlueBook/2013/individual-articles/01\\_Lorenc\\_Andrew\\_EnVar\\_nomenclature.pdf](http://www.wcrp-climate.org/WGNE/BlueBook/2013/individual-articles/01_Lorenc_Andrew_EnVar_nomenclature.pdf).

techniques, but they originate from quite distinct objectives. We will first discuss the *hybrid* methods that consider two DA systems running concurrently (building on already existing systems), but that additionally exchange information in hopes of improving the global performance. Second, we will discuss systems based on an *ensemble of DA*, or *EDA*. It is usually based on an already existing variational system such as a 4D-Var. An ensemble of such 4D-Var is generated with the goal of introducing dynamical errors into the background error covariance matrix of 4D-Var. Third, 4D-EnVar systems stem from the need to avoid the development and maintenance of complex adjoint operators for NWP centers that already operate a 4D-Var. The idea is to perform the 4D variational analysis within the reduced space of a 4D ensemble of model trajectories. Finally, we will discuss the IEnKS, which uses a 4D ensemble of trajectories to perform a nonlinear variational analysis and to represent flow-dependent errors. Its initial goal was to endow the EnKF with the ability to perform nonlinear analysis and generate a consistent updated ensemble, which requires iterating as in the numerical optimization of nonlinear objective functions, and with the ultimate goal of systematically outperforming the EnKF and 4D-Var, especially in strongly nonlinear regimes.

These new DA approaches significantly blur the lines described in the concluding remarks by Kalnay et al. [2007] regarding the future of DA techniques. For challenging DA problems, pure EnKF or pure 4D-Var state-of-the-art systems don't exist any more. These methods have cross-fertilized.

Because this topic of DA is relatively new and rapidly evolving, one must keep in mind that this chapter is a snapshot of the state of the art in early 2016.

## 7.1 ■ The hybrid methods

*Hybrid* could refer to two different concepts that are nevertheless intertwined. Hybrid DA defines a system where two DA methods, usually already implemented, are run concurrently and exchange information about the errors and the estimated model state to get an even better estimation of these. In practice, however, a hybrid DA system combines static and predetermined prior error statistics, such as in OI, 3D-Var, or 4D-Var, with flow-dependent error statistics such as those produced by an EnKF. Consequently, it is actually the error covariances that are hybridized, not necessarily the DA systems. Nonetheless, these two types of error covariances were historically produced by two distinct DA systems (3D-Var and EnKF, typically), so that the second definition is actually often connected to the first.

From this consideration on terminology, one can guess that the goal of this hybridization is to have systems based on OI, 3D-Var, and 4D-Var benefit from a dynamical estimation of the errors and, reciprocally, to have an EnKF system that has a dynamical but degenerate representation of the errors benefit from a full-rank prior representation of all errors. This echoes our initial discussion on the flaws and merits of 4D-Var and of the EnKF.

### 7.1.1 ■ Hybridizing the EnKF and 3D-Var

Here, we shall mostly focus on the hybridization of an EnKF system with a 3D-Var (possibly OI) system. The 3D-Var system relies on a full-rank static (and/or predetermined) error covariance matrix,  $\mathbf{C}$ . The EnKF estimates the flow-dependent errors through the perturbations  $\mathbf{P}^f = \frac{1}{m-1} \sum_{i=1}^m (\mathbf{x}_i - \bar{\mathbf{x}})(\mathbf{x}_i - \bar{\mathbf{x}})^T = \mathbf{X}_f \mathbf{X}_f^T$ , where  $\mathbf{X}_f$  is the normalized anomaly matrix (see Section 6.4). Whatever the type of EnKF, the simplest

idea is to perform a state analysis using a linear combination of these error covariances,

$$\mathbf{B} = \gamma \mathbf{C} + (1 - \gamma) \mathbf{P}^f,$$

where  $\gamma \in [0, 1]$  is a scalar parameter that controls the blending of the covariances: using  $\mathbf{B}$  with  $\gamma = 1$  corresponds to a 3D-Var state analysis, while using  $\mathbf{B}$  with  $\gamma = 0$  corresponds to the pure EnKF state analysis.

If the EnKF is stochastic, then one can update each member,  $i = 1, \dots, m$ , of the ensemble using a state analysis with  $\mathbf{B}$ , which essentially solves the variational problem with the following cost function:

$$\mathcal{L}_i(\mathbf{x}) = \frac{1}{2} \|\mathbf{y} + \boldsymbol{\epsilon}_i - \mathcal{H}(\mathbf{x})\|_{\mathbf{R}}^2 + \frac{1}{2} \|\mathbf{x} - \mathbf{x}_i\|_{\mathbf{B}}^2, \quad (7.1)$$

where  $\mathbf{x}_i$  is the first guess of member  $i$  and  $\boldsymbol{\epsilon}_i$  is a member-dependent perturbation drawn from the observation error prior (see Section 6.3). Recall that  $\|\mathbf{z}\|_{\mathbf{B}}^2 = \mathbf{z}^T \mathbf{B}^{-1} \mathbf{z}$ . The elegance of the scheme lies in the fact that it yields a statistically consistent update of the ensemble thanks to the stochastic representation of errors. This consistency is exact if  $\mathcal{H}$  is linear and approximate otherwise. It was first proposed by Hamill and Snyder [2000]. This EnKF-3D-Var scheme was shown to improve the performance of DA over the EnKF when the ensemble is small, and over 3D-Var when the observation network is not dense enough. Of course, this requires a proper tuning of  $\gamma$ .

If the EnKF is deterministic, the construction of the hybrid is not as straightforward, especially concerning the update of the perturbation ensemble. First, one extracts from the ensemble the mean state and perturbations,  $\{\mathbf{x}_i\}_{i=1, \dots, m} \longrightarrow \bar{\mathbf{x}}, \mathbf{X}_f$ . Second, one can perform an analysis on the mean state, i.e., solve the following variational problem:

$$\mathbf{x}^a = \underset{\mathbf{x}}{\operatorname{argmin}} \mathcal{L}(\mathbf{x}) \quad \text{where} \quad \mathcal{L}(\mathbf{x}) = \frac{1}{2} \|\mathbf{y} - \mathcal{H}(\mathbf{x})\|_{\mathbf{R}}^2 + \frac{1}{2} \|\mathbf{x} - \bar{\mathbf{x}}\|_{\mathbf{B}}^2. \quad (7.2)$$

This mean state analysis is equivalent to that of the hybrid stochastic EnKF-3D-Var (7.1) if the perturbed observations are centered and if  $\mathcal{H}$  is close to being linear.

However, the deterministic update of the perturbations is not as simple as in the stochastic hybrid case. To make it simple, and in the absence of localization of the perturbations, Wang et al. [2007, 2008] advocated using the right-transform perturbations update of the ETKF scheme (see (6.16) of Section 6.4.3):

$$\mathbf{X}_a = \mathbf{X}_f \left( \mathbf{I}_m + \mathbf{Y}_f^T \mathbf{R}^{-1} \mathbf{Y}_f \right)^{-\frac{1}{2}} \mathbf{U}, \quad \text{where} \quad \mathbf{Y}_f = \mathbf{H} \mathbf{X}_f.$$

This is simple but only updates the perturbations based on the knowledge of the dynamical errors, neglecting the static background errors. It is as if  $\gamma$  were set to 0 in the perturbations update step. This may lead to a misestimation of the errors and could require inflation to account for a possible underestimation. These updated perturbations obtained from  $\mathbf{X}_a$  are then added to the state analysis,  $\mathbf{x}^a$ , to obtain the updated ensemble.

However, there are ways to improve these perturbation updates. We saw in Section 6.4.4 that a full-rank left-transform update is also theoretically possible:

$$\mathbf{X}_a = \left( \mathbf{I}_n + \mathbf{B} \mathbf{H}^T \mathbf{R}^{-1} \mathbf{H} \right)^{-\frac{1}{2}} \mathbf{X}_f \mathbf{U}, \quad (7.3)$$

with  $\mathbf{B} = \gamma\mathbf{C} + (1 - \gamma)\mathbf{P}^f$ , which is meant to be full rank. With high-dimensional systems, this inverse square root is not numerically affordable. But it could be estimated using iterative Lanczos-based methods (see Golub and van Loan [2013]) or randomized SVD techniques (see Halko et al. [2011]), because the full-rank left transform acts on the small-dimensional vector subspace of the perturbations,  $\mathbf{X}_f$ .

The perturbations could actually be computed by extracting the dominant modes of the Hessian of the cost function (7.2). This could be achieved using iterative Krylov-based methods [Golub and van Loan, 2013]. Extracting the Lanczos vectors was advocated by T. Auligné and implemented in the EVIL (Ensemble Variational Integrated Lanczos) DA system.

Bocquet et al. [2015] proposed generalizing the left-transform update formula (7.3) of Sakov and Bertino [2011]. This formula is meant to extract some residual information from the static background error statistics that is not accounted for in (7.3) if used in an hybrid system. It reads

$$\mathbf{X}_a = \left[ \mathbf{I}_n + \left( \gamma\mathbf{C} + (1 - \gamma)\mathbf{X}_f\mathbf{X}_f^T \right) \mathbf{H}^T \mathbf{R}^{-1} \mathbf{H} \right]^{-\frac{1}{2}} \left[ (1 - \gamma)\mathbf{I}_n + \gamma\mathbf{X}_f\mathbf{X}_f^\dagger \mathbf{C} (\mathbf{X}_f\mathbf{X}_f^T)^\dagger \right]^{\frac{1}{2}} \mathbf{X}_f \mathbf{U},$$

where  $\dagger$  denotes the Moore–Penrose inverse of a matrix.

Most of the hybrid methods focus on a linear combination of covariance matrices. However, Penny [2014] proposed using a linear combination of Kalman gains that depends in a nontrivial way on the gain that would be obtained from the two DA methods that are part of the hybrid. Penny [2014] defines a hybrid/mean-LETKF: it runs an LETKF to obtain a mean update  $\bar{\mathbf{x}}_a$ , which is used in the subsequent 3D-Var analysis defined by the cost function

$$\mathcal{L}(\mathbf{x}) = \frac{1}{2} \|\mathbf{y} - \mathcal{H}(\mathbf{x})\|_{\mathbf{R}}^2 + \frac{1}{2} \|\mathbf{x} - \bar{\mathbf{x}}_a\|_{\mathbf{C}}^2.$$

The updated ensemble of the LETKF is then recentered on  $\mathbf{x}_{\text{hybrid}}^a = \underset{\mathbf{x}}{\operatorname{argmin}} \mathcal{L}(\mathbf{x})$ .

This was shown to be equivalent to the update

$$\mathbf{x}_{\text{hybrid}}^a = \bar{\mathbf{x}} + \hat{\mathbf{K}}(\mathbf{y} - \mathcal{H}(\bar{\mathbf{x}})), \quad \text{with} \quad \hat{\mathbf{K}} = \mathbf{K} + \gamma\mathbf{K}^C(\mathbf{I}_p - \mathbf{H}\mathbf{K}),$$

where  $\bar{\mathbf{x}}$  is the ensemble mean,

$$\mathbf{K} = \mathbf{P}^f \mathbf{H}^T (\mathbf{H} \mathbf{P}^f \mathbf{H}^T + \mathbf{R})^{-1}$$

is the flow-dependent gain and

$$\mathbf{K}^C = \mathbf{C} \mathbf{H}^T (\mathbf{H} \mathbf{C} \mathbf{H}^T + \mathbf{R})^{-1}$$

is the static gain.

### 7.1.2 ■ Augmented state formalism

The analysis process that results from the blending of several covariances as many sources of statistical information can be represented by the straightforward linear combinations of the covariances. It can also be represented through an augmented state formalism where the analysis increments coming from each part of the combined covariance matrix seem independent. This has been suggested by Lorenc [2003] and Buehner [2005].

The two representations are actually equivalent [Wang et al., 2007]. Let us give a minimal demonstration of this equivalence by only considering the prior of a hybrid analysis where  $\mathbf{B}_1$  and  $\mathbf{B}_2$  are the two background error covariance matrices that are combined. For the sake of simplicity, they are both considered full-rank matrices, but the generalization to the case where one of them is degenerate does not pose any difficulty. Here, the mixing coefficients (such as  $\gamma$ ) are hidden in the definition of  $\mathbf{B}_1$  and  $\mathbf{B}_2$ . The prior term of the cost function reads

$$\mathcal{L}_b(\mathbf{x}) = \frac{1}{2} \|\mathbf{x} - \bar{\mathbf{x}}\|_{\mathbf{B}_1 + \mathbf{B}_2}^2.$$

Introducing the Lagrangian,

$$\mathcal{L}_b(\mathbf{x}, \boldsymbol{\eta}) = \boldsymbol{\eta}^T (\mathbf{x} - \bar{\mathbf{x}}) - \frac{1}{2} \|\boldsymbol{\eta}\|_{(\mathbf{B}_1 + \mathbf{B}_2)^{-1}}^2 = \boldsymbol{\eta}^T (\mathbf{x} - \bar{\mathbf{x}}) - \frac{1}{2} \|\boldsymbol{\eta}\|_{\mathbf{B}_1^{-1}}^2 - \frac{1}{2} \|\boldsymbol{\eta}\|_{\mathbf{B}_2^{-1}}^2,$$

which is a function of  $\mathbf{x}$  and a vector of Lagrange multipliers  $\boldsymbol{\eta}$ , we have

$$\max_{\boldsymbol{\eta}} \mathcal{L}_b(\mathbf{x}, \boldsymbol{\eta}) = \mathcal{L}_b(\mathbf{x}),$$

by simple maximization of a quadratic cost function.

The same trick can be enforced once again but on the two last quadratic terms separately using ancillary variables  $\delta \mathbf{x}_1$  and  $\delta \mathbf{x}_2$ . Denoting

$$\mathcal{L}_b(\mathbf{x}, \boldsymbol{\eta}, \delta \mathbf{x}_1, \delta \mathbf{x}_2) = \boldsymbol{\eta}^T (\mathbf{x} - \bar{\mathbf{x}}) - \boldsymbol{\eta}^T \delta \mathbf{x}_1 + \frac{1}{2} \|\delta \mathbf{x}_1\|_{\mathbf{B}_1}^2 - \boldsymbol{\eta}^T \delta \mathbf{x}_2 + \frac{1}{2} \|\delta \mathbf{x}_2\|_{\mathbf{B}_2}^2,$$

we have

$$\min_{\delta \mathbf{x}_1, \delta \mathbf{x}_2} \mathcal{L}_b(\mathbf{x}, \boldsymbol{\eta}, \delta \mathbf{x}_1, \delta \mathbf{x}_2) = \mathcal{L}_b(\mathbf{x}, \boldsymbol{\eta}).$$

Factorizing on  $\boldsymbol{\eta}$ , we obtain the Lagrangian

$$\mathcal{L}_b(\mathbf{x}, \boldsymbol{\eta}, \delta \mathbf{x}_1, \delta \mathbf{x}_2) = \boldsymbol{\eta}^T (\mathbf{x} - \bar{\mathbf{x}} - \delta \mathbf{x}_1 - \delta \mathbf{x}_2) + \frac{1}{2} \|\delta \mathbf{x}_1\|_{\mathbf{B}_1}^2 + \frac{1}{2} \|\delta \mathbf{x}_2\|_{\mathbf{B}_2}^2,$$

where  $\boldsymbol{\eta}$  clearly plays the role of a vector of Lagrange multipliers, which enforces the constraint  $\mathbf{x} = \bar{\mathbf{x}} + \delta \mathbf{x}_1 + \delta \mathbf{x}_2$ , where  $\delta \mathbf{x}_1$  and  $\delta \mathbf{x}_2$  are two a priori independent increments.

When applied to the full analysis cost function, this yields an optimization problem over  $\delta \mathbf{x}_1$  and  $\delta \mathbf{x}_2$  in place of  $\mathbf{x}$  but under the constraint  $\mathbf{x} = \bar{\mathbf{x}} + \delta \mathbf{x}_1 + \delta \mathbf{x}_2$ . Indeed, we have

$$\begin{aligned} \mathcal{L} &= \min_{\mathbf{x}} \mathcal{L}(\mathbf{x}) \\ &= \min_{\mathbf{x}} \left\{ \frac{1}{2} \|\mathbf{y} - \mathcal{H}(\mathbf{x})\|_{\mathbf{R}}^2 + \mathcal{L}_b(\mathbf{x}) \right\} \\ &= \min_{\mathbf{x}} \left\{ \frac{1}{2} \|\mathbf{y} - \mathcal{H}(\mathbf{x})\|_{\mathbf{R}}^2 + \max_{\boldsymbol{\eta}} \min_{\delta \mathbf{x}_1, \delta \mathbf{x}_2} \mathcal{L}_b(\mathbf{x}, \boldsymbol{\eta}, \delta \mathbf{x}_1, \delta \mathbf{x}_2) \right\} \\ &= \min_{\mathbf{x}, \delta \mathbf{x}_1, \delta \mathbf{x}_2: \mathbf{x} = \bar{\mathbf{x}} + \delta \mathbf{x}_1 + \delta \mathbf{x}_2} \left\{ \frac{1}{2} \|\mathbf{y} - \mathcal{H}(\mathbf{x})\|_{\mathbf{R}}^2 + \frac{1}{2} \|\delta \mathbf{x}_1\|_{\mathbf{B}_1}^2 + \frac{1}{2} \|\delta \mathbf{x}_2\|_{\mathbf{B}_2}^2 \right\} \\ &= \min_{\delta \mathbf{x}_1, \delta \mathbf{x}_2} \left\{ \frac{1}{2} \|\mathbf{y} - \mathcal{H}(\bar{\mathbf{x}} + \delta \mathbf{x}_1 + \delta \mathbf{x}_2)\|_{\mathbf{R}}^2 + \frac{1}{2} \|\delta \mathbf{x}_1\|_{\mathbf{B}_1}^2 + \frac{1}{2} \|\delta \mathbf{x}_2\|_{\mathbf{B}_2}^2 \right\} \\ &= \min_{\delta \mathbf{x}_1, \delta \mathbf{x}_2} \mathcal{L}(\delta \mathbf{x}_1, \delta \mathbf{x}_2). \end{aligned} \tag{7.4}$$

This proves the equivalence between minimizing  $\mathcal{L}(\mathbf{x})$  and minimizing  $\mathcal{L}(\delta \mathbf{x}_1, \delta \mathbf{x}_2)$ , which is defined by the last equality of (7.4).

One advantage of this augmented state representation is that a preconditioned variational problem for  $\mathcal{L}(\delta \mathbf{x}_1, \delta \mathbf{x}_2)$  can be obtained more easily. For instance, if we use  $\mathbf{B} = \gamma \mathbf{C} + (1 - \gamma) \mathbf{X}_f \mathbf{X}_f^T$ , and assuming we know a square root of  $\mathbf{C}$ , we can obtain the equivalent augmented state cost function

$$\mathcal{L}(\delta \mathbf{x}_c, \mathbf{w}) = \frac{1}{2} \left\| \mathbf{y} - \mathcal{H} \left( \bar{\mathbf{x}} + \sqrt{\gamma} \mathbf{C}^{\frac{1}{2}} \delta \mathbf{x}_c + \sqrt{1 - \gamma} \mathbf{X}_f \mathbf{w} \right) \right\|_{\mathbf{R}}^2 + \frac{1}{2} \|\delta \mathbf{x}_c\|^2 + \frac{1}{2} \|\mathbf{w}\|^2,$$

where  $\|\mathbf{z}\|^2 = \mathbf{z}^T \mathbf{z}$ . This cost function may be much more efficiently minimized than

$$\mathcal{L}(\mathbf{x}) = \frac{1}{2} \|\mathbf{y} - \mathcal{H}(\mathbf{x})\|_{\mathbf{R}}^2 + \frac{1}{2} \|\mathbf{x} - \bar{\mathbf{x}}\|_{\gamma \mathbf{C} + (1 - \gamma) \mathbf{X}_f \mathbf{X}_f^T}^2$$

because of the preconditioning of  $\delta \mathbf{x}_c$  and  $\mathbf{w}$ .

### 7.1.3 ■ Localization of the perturbations

As can be seen from  $\mathbf{B} = \gamma \mathbf{C} + (1 - \gamma) \mathbf{X}_f \mathbf{X}_f^T$ , the effective background error covariance matrix is full rank as long as the static prior remains nondegenerate, even if the ensemble size is small. This actually performs a kind of localization called *shrinkage* in statistics. That is why an EnKF can be made robust by this hybridization even if the ensemble is small and even in the absence of the main localization techniques that we discussed in Chapter 6 [Hamill and Snyder, 2000; Wang et al., 2007]. However, in theory and in practice, shrinkage does not seem as efficient as localization for geophysical models. It is therefore useful to further localize the perturbations in the combined covariance matrix  $\mathbf{B}$  with

$$\mathbf{B} = \gamma \mathbf{C} + (1 - \gamma) \rho \circ (\mathbf{X}_f \mathbf{X}_f^T),$$

using covariance localization by a Schur product with a short-range correlation matrix  $\rho$  (see Section 6.5.1.2). The variational analysis is then based on the cost function

$$\mathcal{L}(\mathbf{x}) = \frac{1}{2} \|\mathbf{y} - \mathcal{H}(\mathbf{x})\|_{\mathbf{R}}^2 + \frac{1}{2} \|\mathbf{x} - \bar{\mathbf{x}}\|_{\gamma \mathbf{C} + (1 - \gamma) \rho \circ (\mathbf{X}_f \mathbf{X}_f^T)}^2. \quad (7.5)$$

The augmented-state trick can be used to separate the increments that project onto the static background error covariance matrix and onto the localized sampled error covariance matrix, as follows:

$$\begin{aligned} \mathcal{L}(\delta \mathbf{x}_c, \delta \mathbf{x}_p) &= \frac{1}{2} \left\| \mathbf{y} - \mathcal{H}(\bar{\mathbf{x}} + \delta \mathbf{x}_c + \delta \mathbf{x}_p) \right\|_{\mathbf{R}}^2 \\ &\quad + \frac{1}{2} \|\delta \mathbf{x}_c\|_{\gamma \mathbf{C}}^2 + \frac{1}{2} \left\| \delta \mathbf{x}_p \right\|_{(1 - \gamma) \rho \circ (\mathbf{X}_f \mathbf{X}_f^T)}^2. \end{aligned}$$

Then, we can reuse the  $\alpha$  control variable trick of Section 6.7.2.3 on the flow-dependent part of the background error covariances. We note that this  $\alpha$  control variable trick can actually be seen as an augmented spacewise state representation. We obtain

$$\begin{aligned} \mathcal{L}(\delta \mathbf{x}_c, \alpha) &= \frac{1}{2} \left\| \mathbf{y} - \mathcal{H} \left( \bar{\mathbf{x}} + \delta \mathbf{x}_c + \sum_{i=1}^m \alpha_i \circ [\mathbf{X}_f]_i \right) \right\|_{\mathbf{R}}^2 \\ &\quad + \frac{1}{2} \|\delta \mathbf{x}_c\|_{\gamma \mathbf{C}}^2 + \frac{1}{2} \sum_{i=1}^m \|\alpha_i\|_{(1 - \gamma) \rho}^2. \end{aligned}$$



Recall that  $\alpha = [\alpha_1, \dots, \alpha_m]$  can be viewed as a matrix of size  $n \times m$ , and that  $[\mathbf{X}_f]_i$  is the  $i$ th perturbation of the normalized perturbation matrix  $\mathbf{X}_f$ . With preconditioning, one finally obtains

$$\begin{aligned} \mathcal{L}(\delta \mathbf{x}_c, \alpha) = & \frac{1}{2} \left\| \mathbf{y} - \mathcal{H} \left( \bar{\mathbf{x}} + \sqrt{\gamma} \mathbf{C}^{\frac{1}{2}} \delta \mathbf{x}_c + \sqrt{1-\gamma} \rho^{\frac{1}{2}} \sum_{i=1}^m \alpha_i \circ [\mathbf{X}_f]_i \right) \right\|_{\mathbf{R}}^2 \\ & + \frac{1}{2} \|\delta \mathbf{x}_c\|^2 + \frac{1}{2} \sum_{i=1}^m \|\alpha_i\|^2. \end{aligned}$$

This representation, which was first advocated by Lorenc [2003] and Buehner [2005], implies that the solution is parameterized as

$$\mathbf{x} = \bar{\mathbf{x}} + \sqrt{\gamma} \mathbf{C}^{\frac{1}{2}} \delta \mathbf{x}_c + \sqrt{1-\gamma} \rho^{\frac{1}{2}} \sum_{i=1}^m \alpha_i \circ [\mathbf{X}_f]_i.$$

## 7.2 ■ Ensemble of variational data assimilations (EDA)

Another class of hybrid systems stems from NWP centers where 4D-Var is in use. It consists of processing an *ensemble of data assimilations* or *EDA*. More generally, an EDA system denotes a DA system that processes several variational analyses in parallel. The goal is to introduce some flow dependence in the 4D-Var operational schemes that were initially only based on the static background error covariance matrix. This scheme actually closely mimics the stochastic EnKF and, even more to the point, the hybrid EnKF-3D-Var scheme introduced by Hamill and Snyder [2000] and described earlier.

The main idea is to maintain an ensemble of Var, which will be assumed to be a 4D-Var in the following. This is usually numerically costly for 4D-Var and may require degrading model resolution. Each analysis uses the same static background error covariance matrix  $\mathbf{B}$ , which may have been obtained from the sampled covariances whose variances have been properly filtered and whose correlations have been regularized, as well as the static background covariances [Raynaud et al., 2009; Berre and Desroziers, 2010]. Just as in the stochastic EnKF, it is necessary for each analysis to have perturbed observations to maintain statistical consistency (Section 6.3). The strong-constraint 4D-Var cost function for each analysis,  $i = 1, \dots, m$ , has the form

$$\mathcal{L}_i(\mathbf{x}_0) = \frac{1}{2} \sum_{k=0}^K \left\| \mathbf{y}_k + \epsilon_k^i - \mathcal{H}_k \circ \mathcal{M}_{k:0}(\mathbf{x}_0) \right\|_{\mathbf{R}_k}^2 + \frac{1}{2} \left\| \mathbf{x}_0 - \mathbf{x}_0^i \right\|_{\mathbf{B}}^2,$$

where  $\mathcal{M}_{k:0}$  is the resolvent of the forecast model from  $t_0$  to  $t_k$ ,  $\mathcal{H}_k$  is the observation operator at  $t_k$ , and  $\epsilon_k^i$  is the random noise added to observation  $\mathbf{y}_k$  and is related to the  $i$ th member analysis. The symbol  $\circ$  stands for the composition operator. This generates an ensemble of updates, one for each  $\mathbf{x}_0^i$ , similarly to the stochastic EnKF. It is also possible to perturb each member of the ensemble in the forecast step to account for (parametric or not) model error. Hence, the ensemble will be instrumental in accounting for flow dependence and model error.

This methodology has been implemented at Météo-France [Raynaud et al., 2009; Berre and Desroziers, 2010; Berre et al., 2015] as well as at the ECMWF [Bonavita et al., 2011, 2012] to enhance their 4D-Var system and to introduce flow dependence



of the errors. From a mathematical standpoint, their operational 4D-Var is now quite close to a hybrid DA system based on a stochastic EnKF. The regularization techniques parallel those used in the EnKF: inflation and localization. The localization is, however, enforced via a regularization based on wavelets [Berre et al., 2015], a technique that has been long perfected in operational 4D-Var at the ECMWF and Météo-France.

As a rather consistent stochastic sampling method, an ensemble of 4D-Vars following the EDA scheme is likely to approximately sample from the Bayesian conditional distribution of the DA problem over the 4D-Var DAW. M. Jardak and O. Talagrand have numerically shown that a single analysis of such an EDA approach leads to a reliable updated ensemble and a quasi-flat rank diagram histogram, which supports the seemingly Bayesian character of the EDA sampling (personal communication).

## 7.3 ■ 4D-EnVar

The primary goal of NWP centers that already use 4D-Var (the ECMWF, the UK Met-Office, Météo-France, Environment Canada, the Japan Meteorological Agency) has been to circumvent the derivation and maintenance of the tangent linear and adjoint forecast models. A secondary goal has been to incorporate flow dependence into 4D-Var. As we have seen, this second objective can be achieved using an EDA system that essentially mimics the stochastic EnKF.

### 7.3.1 ■ A 4D-Var without the forecast model adjoint

A solution for the first problem draws its inspiration from the elegant way the EnKF handles the tangent linear and adjoint of the observation operator. We saw in Chapter 6 that any occurrence of the error statistics or any regression coefficient that involves the tangent linear of the observation operator can be estimated thanks to the ensemble of perturbations. For instance, recalling (6.11) from Section 6.3.3,

$$\begin{aligned}\bar{\mathbf{y}}^f &= \frac{1}{m} \sum_{i=1}^m \mathcal{H}(\mathbf{x}_i^f), \\ \mathbf{P}^f \mathbf{H}^T &\simeq \frac{1}{m-1} \sum_{i=1}^m (\mathbf{x}_i^f - \bar{\mathbf{x}}^f) [\mathcal{H}(\mathbf{x}_i^f) - \bar{\mathbf{y}}^f]^T, \\ \mathbf{H} \mathbf{P}^f \mathbf{H}^T &\simeq \frac{1}{m-1} \sum_{i=1}^m [\mathcal{H}(\mathbf{x}_i^f) - \bar{\mathbf{y}}^f] [\mathcal{H}(\mathbf{x}_i^f) - \bar{\mathbf{y}}^f]^T.\end{aligned}$$

In a 4D-Var, we are also concerned with the sensitivities to observations within the DAW to the initial state vector. These are typically related to the asynchronous and synchronous statistics  $\mathbf{P}_0^f (\mathbf{H}_k \mathbf{M}_{k:0})^T$  and  $(\mathbf{H}_k \mathbf{M}_{k:0}) \mathbf{P}_0^f (\mathbf{H}_k \mathbf{M}_{k:0})^T$ , respectively, where  $\mathbf{M}_{k:0}$  is the tangent linear of the forecast model that relates an error at the beginning of the DAW, i.e., at  $t_0$ , to an error within the DAW, at  $t_k$ , whereas  $\mathbf{H}_k \mathbf{M}_{k:0}$  relates an error,  $t_0$ , to an observation error within the DAW.

Using a similar trick as in the EnKF, Liu et al. [2008] proposed using the ensemble to estimate these sensitivities within the DAW, which, in the absence of the ensemble, would require the adjoint models. The ensemble is forecast within the DAW, with  $\mathcal{H}_k \circ \mathcal{M}_{k:0}$  playing the role of  $\mathcal{H}_k$  in the EnKF. In essence, the adjoint can be computed in this scheme because it is estimated from the tangent linear by an ansatz of the finite differences, and because the action of the model within the ensemble subspace can easily be represented by a matrix whose adjoint is simply the matrix transpose operator.

Therefore, to avoid the use of the adjoint in a 4D-Var, one could perform the variational optimization in the reduced basis of the ensemble perturbations. This idea clearly borrows from the reduced-order 4D-Vars developed in ocean DA [Robert et al., 2005, 2006a], which avoid the use of the adjoint model and offer an efficient preconditioning for the minimization (see Section 5.4.2).

More precisely, let us start with the 4D-Var cost function over the DAW  $[t_0, t_K]$ ,

$$\mathcal{L}(\mathbf{x}_0) = \frac{1}{2} \sum_{k=0}^K \|\mathbf{y}_k - \mathcal{F}_{k:0}(\mathbf{x}_0)\|_{\mathbf{R}_k}^2 + \frac{1}{2} \|\mathbf{x}_0 - \bar{\mathbf{x}}_0\|_{\mathbf{P}^f}^2,$$

where observations at  $t_0, t_1, \dots, t_K$  are assimilated. We have defined  $\mathcal{F}_{k:0} = \mathcal{H}_k \circ \mathcal{M}_{k:0}$ , where  $\circ$  stands for the composition of operators. Suppose that the background error covariance matrix is sampled from an ensemble of centered perturbations,  $\mathbf{P}^f = \mathbf{X}_f \mathbf{X}_f^T$ . Following the ETKF construction (see Chapter 6), we look for a solution in the affine subspace generated by  $\bar{\mathbf{x}}_0$  and the perturbations  $\mathbf{X}_f$ ,

$$\mathbf{x}_0 = \bar{\mathbf{x}}_0 + \mathbf{X}_f \mathbf{w}.$$

The goal is to minimize the reduced-order cost function

$$\mathcal{L}(\mathbf{w}) = \frac{1}{2} \sum_{k=0}^K \|\mathbf{y}_k - \mathcal{F}_{k:0}(\bar{\mathbf{x}}_0 + \mathbf{X}_f \mathbf{w})\|_{\mathbf{R}_k}^2 + \frac{1}{2} \|\mathbf{w}\|^2,$$

whose quadratic approximation obtained by linearizing around the first guess is

$$\mathcal{L}(\mathbf{w}) \simeq \frac{1}{2} \sum_{k=0}^K \|\mathbf{y}_k - \mathcal{F}_{k:0}(\bar{\mathbf{x}}_0) + \mathbf{H}_k \mathbf{M}_{k:0} \mathbf{X}_f \mathbf{w}\|_{\mathbf{R}_k}^2 + \frac{1}{2} \|\mathbf{w}\|^2.$$

The argument of the minimum of this cost function is

$$\mathbf{w}^a = \left[ \mathbf{I}_m + \sum_{k=0}^K (\mathbf{H}_k \mathbf{M}_{k:0} \mathbf{X}_f)^T \mathbf{R}_k^{-1} (\mathbf{H}_k \mathbf{M}_{k:0} \mathbf{X}_f) \right]^{-1} \sum_{k=0}^K (\mathbf{H}_k \mathbf{M}_{k:0} \mathbf{X}_f)^T \mathbf{R}_k^{-1} (\mathbf{y}_k - \mathcal{F}_{k:0}(\bar{\mathbf{x}}_0)).$$

The key point is that  $\mathbf{H}_k \mathbf{M}_{k:0} \mathbf{X}_f$ , as well as its transpose matrix, can be estimated with a single ensemble forecast through the DAW,

$$\mathbf{H}_k \mathbf{M}_{k:0} \mathbf{X}_f \approx \frac{1}{\varepsilon} \mathcal{F}_{k:0}(\bar{\mathbf{x}}_0 \mathbf{1}^T + \varepsilon \mathbf{X}_f) \left( \mathbf{I}_m - \frac{\mathbf{1} \mathbf{1}^T}{m} \right), \quad (7.6)$$

where  $0 < \varepsilon \ll 1$  is a small scaling parameter needed to compute the finite differences. These can also be estimated by choosing  $\varepsilon = 1$  if the ensemble spread is small enough.

This stands as the analysis step of the method that is now commonly called *4D-EnVar*, where  $\varepsilon = 1$  is chosen to minimize the number of ensemble forecasts. It can hardly be seen as a new DA method as it is based on or revisits already-known techniques such as reduced-order 4D-Var. But it does stand as a class of implementation techniques meant to circumvent the use of the adjoint model in the 4D-Var, and possibly as in EDA systems to incorporate flow-dependent errors.

### 7.3.2 ■ Variants

Another ingredient needed to fully specify a 4D-EnVar scheme is the choice of the perturbations. In Liu et al. [2009] and Buehner et al. [2010a], the perturbations were

obtained from a stochastic EnKF similarly to Hamill and Snyder [2000]. This introduced the flow dependence of the errors. Quite often, the 4D-EnVar performs variational analysis using the perturbations generated by an independent EnKF implementation. If the updated perturbations are obtained deterministically from an ETKF-like update formula derived from the main variational analysis, rather than from an independent EnKF running concurrently, then this DA scheme actually mathematically coincides with the so-called 4D-LETKF [Hunt et al., 2004; Fertig et al., 2007].

If an adjoint model used in the original 4D-Var system is available and if the focus is more on building an EnVar to represent the flow dependence of the errors, then the method is usually referred to as a *4D-Var-Ben* [Buehner et al., 2010a,b], emphasizing that the method still resembles a 4D-Var where the background error covariance matrix has been obtained from an ensemble.

In Section 7.1, we mostly focused on the hybridization of an EnKF with a 3D-Var. A similar approach can be implemented but with a 4D-Var [Zhang and Zhang, 2012; Clayton et al., 2013]. Again the scheme mainly relies on an EnKF. A 4D variational optimization is performed for state estimation using the combination of a static background covariance matrix and the flow-dependent sampled covariances of the EnKF. The latter can be localized using, for instance, a 4D generalization of the  $\alpha$  control variable trick. This yields a state analysis. The updated ensemble is built on the updated ensemble of the EnKF but centered on the variational state analysis. Similar to 4D-Var-Ben, this EnVar approach benefits from the available adjoint of the 4D-Var.

To generate updated perturbations in an EDA system where a single state analysis is obtained from a 4D-EnVar, one would have to consider an ensemble of 4D-EnVar, an option that is considered at the UK MetOffice [Lorenc et al., 2015].

### 7.3.3 ■ Localization and weak-constraint formalism

The main drawback of performing the four-dimensional variational analysis within the ensemble subspace is that, as for any ensemble-based method, it is likely to be rank deficient with realistic high-dimensional models. That is why localization is mandatory. Unfortunately, spatial localization in such a 4D context is not as simple as in a 3D context, where covariance localization only requires the definition of a proper localization matrix, usually the direct product of horizontal and vertical correlation functions. With the inclusion of the time component, one needs to be able to localize covariances such as  $\mathbf{X}_0 \mathbf{Y}_k^T$  between state variables at  $t_0$  and observations at  $t_k$  within the DAW, as well as  $\mathbf{Y}_k \mathbf{Y}_k^T$  between observations at  $t_k$  within the DAW. It is sound to assume that one can localize the background error covariance matrix at  $t_0$ ,  $\mathbf{X}_0 \mathbf{X}_0^T \mapsto \rho \circ (\mathbf{X}_0 \mathbf{X}_0^T)$ , using the localization matrix  $\rho$  defined at the beginning of the DAW. But the regularization of covariances such as  $\mathbf{X}_0 \mathbf{Y}_k^T$ ,  $\mathbf{Y}_k \mathbf{Y}_k^T$  is not as straightforward. Indeed, the model flow and a static localization operator (here a Schur product) do not commute in general, i.e.,

$$\mathbf{M}_{k:0} (\rho \circ \mathbf{P}_0) \mathbf{M}_{k:0}^T \neq \rho \circ (\mathbf{M}_{k:0} \mathbf{P}_0 \mathbf{M}_{k:0}^T), \quad (7.7)$$

as emphasized in Fairbairn et al. [2014] and Bocquet and Sakov [2014].

Assuming that the model is perfect, and that a spatial localization operator is defined at the beginning of the DAW at  $t_0$ , it is formally possible to derive the equation that governs the dynamics of the localization operator [Bocquet, 2016]. Let us

consider a *linear* localization operator that applies to covariances,  $\mathbb{L} : \mathbf{P} \mapsto \mathbb{L} \cdot \mathbf{P}$ . Schur localization is an example of such a generic linear operator. The transport of the covariances by the TLM from  $t$  to  $t + \delta t$  is formalized with the linear operator

$$\mathcal{T}_{t+\delta t:t} : \mathbf{P}_t \mapsto \mathcal{T}_{t+\delta t:t} \cdot \mathbf{P}_t = \mathbf{M}_{t+\delta t:t} \mathbf{P}_t \mathbf{M}_{t+\delta t:t}^T.$$

Assuming that the localization operator evolves in time, we wish to impose that localization commutes with the TLM, which can be written as

$$\mathcal{T}_{t+\delta t:t} \cdot \mathbb{L}_t \cdot \mathbf{P}_t = \mathbb{L}_{t+\delta t} \cdot \mathcal{T}_{t+\delta t:t} \cdot \mathbf{P}_t. \quad (7.8)$$

Ideally, this dynamical constraint should apply to any  $t$ ,  $\delta t$ , and  $\mathbf{P}_t$ . In the limit where  $\delta t$  goes to zero, the transport operator can be expanded as

$$\mathcal{T}_{t+\delta t:t} = \mathbf{I} \otimes \mathbf{I} + \mathcal{K}_t \delta t + o(\delta t),$$

where  $\mathcal{K}_t$  is a linear operator that can be written  $\mathcal{K}_t = \mathbf{M}_t \otimes \mathbf{I} + \mathbf{I} \otimes \mathbf{M}_t$  and  $\mathbf{I} \otimes \mathbf{I}$  is the identity operator in the space of the covariance matrices. As a consequence, (7.8) can in turn be expanded in the  $\delta t \rightarrow 0$  limit to yield

$$\frac{\partial \mathbb{L}_t}{\partial t} = [\mathcal{K}_t, \mathbb{L}_t], \quad (7.9)$$

where  $[A, B] = AB - BA$  is the commutator of operators. Formally,  $\mathbb{L}_t$  actually acts on  $\text{vec}(\mathbf{P}_t)$ , i.e., the vector formed by the stacked columns of  $\mathbf{P}_t$ . This (quantum) *Liouville equation* prescribes the dynamics of a consistent localization operator for synchronous covariances of the form  $\mathbf{Y}_k \mathbf{Y}_k^T$ . A consistent asynchronous localization operator that can be used to regularize covariances such as  $\mathbf{X}_0 \mathbf{Y}_k^T$  is also needed. In this case, the same Liouville equation still applies but with an asymmetrical transport  $\mathcal{K}_t = \mathbf{I} \otimes \mathbf{M}_t$  (or  $\mathcal{K}_t = \mathbf{M}_t \otimes \mathbf{I}$  for  $\mathbf{Y}_k \mathbf{X}_0^T$ ).

An exact solution to this equation can only be obtained in restrictive cases, for instance when the dynamics of the system are governed by a hyperbolic PDE, which can be solved using characteristic curves. This is not a realistic assumption but it is hoped to be a reliable approximation. In any case, localization should be *covariant* with the flow as much as possible.

This view does suggest a way to localize the perturbations within the DAW more consistently than using a static localization operator. The ensemble should be forecast exactly within the DAW, while the localization operator should be propagated using a surrogate model of advection [Bocquet, 2016; Desroziers et al., 2016]. The cost of the surrogate model of advection is small since an *embarrassingly* parallel Lagrangian transport scheme can be implemented. If the main model represents to some extent the transport of, for instance, potential vorticity, the advection field of the surrogate model could be identified with the wind field of the main model, or a filtered output of this wind field. This approximate covariant localization scheme within the DAW of a 4D-EnVar has a counterpart when using domain localization that involves pulling back the locations of the in situ observations within the DAW to  $t_0$  using a simple Lagrangian model of advection [Bocquet, 2016].

The advantage of hybrid ensemble-4DVar or 4D-Var-Ben systems that do maintain an adjoint model in comparison to 4D-EnVar systems is that covariance localization within the DAW is much easier. Indeed, the minimization can be performed using the

full-rank localized background error covariance matrix thanks to the adjoint model [Fairbairn et al., 2014; Poterjoy and Zhang, 2015; Bocquet, 2016].

A weak-constraint formalism for 4DVar has not been investigated thoroughly so far. However, a formal basis was established by Desroziers et al. [2014]. In particular, a clear connection was established between a weak-constraint 4DVar and a weak-constraint 4DVar, which opens the way to parallelization in time of 4DVar implementations [Fisher et al., 2011].

### 7.3.4 ■ A replacement for 4DVar?

The 4DVar systems have been evaluated and sometimes validated by meteorologists in NWP centers. Quite often, their first goal, which was to achieve similar performance to 4D-Var, has been reached [Buehner et al., 2013; Gustafsson et al., 2014; Lorenc et al., 2015; Kleist and Ide, 2015; Buehner et al., 2015]. This often applies to synoptical scale meteorology, which is rather well observed so that the DA system has error statistics that are quite close to Gaussian. In particular, the EnVar and hybrid methods discussed so far did not rely on an outer loop. However, as suggested in the introduction of this chapter, EnVar methods have more generally the potential to systematically outperform both 4D-Var and EnKF systems. This will be discussed in the next section.

## 7.4 ■ The iterative ensemble Kalman smoother (IEnKS)

The hybrid and EnVar methods described so far have not been derived from first principles. In the following, we shall describe another EnVar method, the iterative ensemble Kalman smoother (IEnKS), which can be heuristically derived from Bayes' rule. As a consequence, all approximations and sources of suboptimality in the scheme are known and accounted for. Moreover, because of this derivation, the scheme is heuristically guaranteed to outperform 4D-Var and the EnKF in terms of precision, regardless of the numerical cost. It can either estimate the tangent linear and adjoint models, like 4DVar, or it can make use of already available tangent and adjoint models, like En4DVar and 4D-Var-Ben. We shall mostly suppose here that the tangent linear and adjoint models are not available.

The IEnKS was introduced and justified through a Bayesian derivation in Bocquet and Sakov [2014]. Here, we shall focus on the description of the algorithm. The IEnKS extends to a 4D-variational analysis the so-called iterative ensemble Kalman filter (IEnKF) of Sakov et al. [2012]. The IEnKS was named after the paper by Bell [1994], who first described such an algorithm in the Kalman filter context. The IEnKS is meant not only for smoothing but also for filtering as well as for forecasting.

In the following, we first precisely describe a simple variant of the algorithm. Here, we shall not be concerned with hybrid covariances. We will only consider flow-dependent errors estimated by the perturbations of an ensemble. Moreover, we shall assume that the model is perfect, as in most implementations of 4D-Var, although weak-constraint generalizations of the IEnKS are possible.

### 7.4.1 ■ The algorithm

As in Section 7.2, we assume that batches of observations,  $\mathbf{y}_k \in \mathbb{R}^{p_k}$ , are collected every  $\Delta t$ , at times  $t_k$ . The observations are related to the state vector through a possibly nonlinear, possibly time-dependent observation operator  $\mathcal{H}_k$ . The observation errors

are assumed to be Gaussian-distributed, unbiased, and uncorrelated in time, with observation error covariance matrices  $\mathbf{R}_k$ .

#### 7.4.1.1 ■ Analysis step

Let us first consider the analysis step of the scheme. It is performed over a window of  $L$  intervals of length  $\Delta t$  ( $L\Delta t$  in time units). By convention, the time at the end of the DAW will be called  $t_L$ , while the time at the beginning of the DAW will be called  $t_0$ . At  $t_0$  (i.e.,  $L\Delta t$  in the past), the prior distribution is estimated from an ensemble of  $m$  state vectors of  $\mathbb{R}^n$ :  $\mathbf{x}_{0,[1]}, \dots, \mathbf{x}_{0,[i]}, \dots, \mathbf{x}_{0,[m]}$ . Index 0 refers to time, while  $[i]$  refers to the ensemble member index. They can be gathered into the ensemble matrix  $\mathbf{E}_0 = [\mathbf{x}_{0,[1]}, \dots, \mathbf{x}_{0,[m]}]$  of size  $n \times m$ . The ensemble can equivalently be given in terms of its mean,  $\bar{\mathbf{x}}_0 = \frac{1}{m} \sum_{i=1}^m \mathbf{x}_{0,[i]}$ , and its (normalized) anomaly matrix,  $\mathbf{X}_0 = \frac{1}{\sqrt{m-1}} [\mathbf{x}_{0,[1]} - \bar{\mathbf{x}}_0, \dots, \mathbf{x}_{0,[m]} - \bar{\mathbf{x}}_0]$ .

As in the EnKF, this prior is modeled as a Gaussian distribution of mean  $\bar{\mathbf{x}}_0$  and covariance matrix  $\mathbf{X}_0 \mathbf{X}_0^T$ , the first- and second-order sampled moments of the ensemble. The background is rarely full rank since the anomalies of the ensemble span a vector space of dimension smaller than or equal to  $m-1$  and in a realistic context  $m \ll n$ . Hence, in the absence of localization, one seeks an analysis state vector  $\mathbf{x}_0$  in the ensemble subspace  $\bar{\mathbf{x}}_0 + \text{Vec} \{ \mathbf{x}_{[1]} - \bar{\mathbf{x}}_0, \dots, \mathbf{x}_{[m]} - \bar{\mathbf{x}}_0 \}$  that can be written  $\mathbf{x}_0 = \bar{\mathbf{x}}_0 + \mathbf{X}_0 \mathbf{w}$ , where  $\mathbf{w}$  is a vector of coefficients in  $\mathbb{R}^m$ . The analysis will be defined as the most likely deterministic state of a cost function in the reduced subspace of the ensemble and will later be identified as the mean of the analysis ensemble.

As in Section 7.3,  $\mathcal{F}_{k:0}$  stands for the composition of  $\mathcal{H}_k$  and the resolvent  $\mathcal{M}_{k:0}$ . The variational analysis of the IEnKS over  $[t_0, t_L]$  stems from a cost function. The restriction of this cost function to the ensemble subspace reads

$$\mathcal{J}(\mathbf{w}) = \sum_{k=L-S+1}^L \frac{1}{2} \|\mathbf{y}_k - \mathcal{F}_{k:0}(\bar{\mathbf{x}}_0 + \mathbf{X}_0 \mathbf{w})\|_{\mathbf{R}_k}^2 + \frac{1}{2} \|\mathbf{w}\|^2. \quad (7.10)$$

The second term represents the prior in ensemble subspace [Hunt et al., 2007]. Here  $S$  batches of observations are assimilated in this analysis. The case  $L=0$ ,  $S=1$ , where  $\mathcal{M}_{0:0}$  is defined as the identity, corresponds to the MLEF that we described in Section 6.7.2.1; the case  $L=1$ ,  $S=1$  corresponds to the IEnKF [Sakov et al., 2012]. Otherwise, one has  $1 \leq S \leq L+1$  and a 4D variational analysis.

This cost function is iteratively minimized in the reduced subspace of the ensemble following a Gauss–Newton algorithm,

$$\mathbf{w}^{(j+1)} = \mathbf{w}^{(j)} - \mathbf{H}_{(j)}^{-1} \nabla \mathcal{J}_{(j)}(\mathbf{w}^{(j)}), \quad (7.11)$$

using the gradient  $\nabla \mathcal{J}$  and an approximation,  $\mathbf{H}$ , of the Hessian in reduced space,

$$\begin{aligned} \mathbf{x}_0^{(j)} &= \bar{\mathbf{x}}_0 + \mathbf{X}_0 \mathbf{w}^{(j)}, \\ \nabla \mathcal{J}_{(j)} &= \mathbf{w}^{(j)} - \sum_{k=L-S+1}^L \mathbf{Y}_{k,(j)}^T \mathbf{R}_k^{-1} [\mathbf{y}_k - \mathcal{F}_{k:0}(\mathbf{x}_0^{(j)})], \\ \mathbf{H}_{(j)} &= \mathbf{I}_m + \sum_{k=L-S+1}^L \mathbf{Y}_{k,(j)}^T \mathbf{R}_k^{-1} \mathbf{Y}_{k,(j)}. \end{aligned}$$



The notation  $(j)$  refers to the iteration index of the minimization. At the first iteration, one sets  $\mathbf{w}^{(0)} = \mathbf{0}$  so that  $\mathbf{x}_0^{(0)} = \bar{\mathbf{x}}_0$ . Recall that  $\mathbf{I}_m$  is the identity matrix in  $\mathbb{R}^m$ . Then  $\mathbf{Y}_{k,(j)} = [\mathcal{F}_{k:0}]'_{\mathbf{x}_0^{(j)}} \mathbf{X}_0$  is the tangent linear of the operator from  $\mathbb{R}^m$  to the observation space. Each iteration solves the inner loop quadratic minimization problem with cost function

$$\mathcal{J}_{(j)}(\mathbf{w}) = \sum_{k=L-S+1}^L \frac{1}{2} \left\| \mathbf{y}_k - \mathcal{F}_{k:0}(\mathbf{x}^{(j)}) - \mathbf{Y}_{k,(j)}(\mathbf{w} - \mathbf{w}^{(j)}) \right\|_{\mathbf{R}_k}^2 + \frac{1}{2} \left\| \mathbf{w} - \mathbf{w}^{(j)} \right\|^2.$$

Here, this inner loop problem is directly dealt with by solving the associated linear system. An elegant idea is to solve it instead using the EnKS [Mandel et al., 2015].

Note that other iterative minimization schemes could be used in place of Gauss–Newton, such as quasi-Newton, Levenberg–Marquardt, or trust-region methods [Bocquet and Sakov, 2012; Mandel et al., 2015; Nino Ruiz and Sandu, 2016], with distinct convergence properties.

The estimation of these sensitivities using the ensemble avoids the use of the model adjoint. These sensitivities can be computed using finite differences (the so-called bundle IEnKS variant). The ensemble is rescaled closer to the mean trajectory by a factor  $\varepsilon$ . It is then propagated through the model and the observation operator ( $\mathcal{F}_{k:0}$ ), after which it is rescaled back by the inverse factor  $\varepsilon^{-1}$ . Following (7.6), this can be written

$$\mathbf{Y}_{k,(j)} \approx \frac{1}{\varepsilon} \mathcal{F}_{k:0} \left( \mathbf{x}_0^{(j)} \mathbf{1}^T + \varepsilon \mathbf{X}_0 \right) \left( \mathbf{I}_m - \frac{\mathbf{1} \mathbf{1}^T}{m} \right), \quad (7.12)$$

where  $\mathbf{1} = (1, \dots, 1)^T \in \mathbb{R}^m$ . Note that the  $\sqrt{m-1}$  factor needed to scale the anomalies has been incorporated in  $\varepsilon$ . It is also possible to compute these sensitivities without resorting to finite differences, choosing  $\varepsilon = 1$ , with very similar IEnKS performance, which is the so-called transform variant [Sakov et al., 2012; Bocquet and Sakov, 2014]. In this alternative, the sensitivities are computed similarly to a 4DEnVar. But this goes further, since  $\varepsilon = 1$  can be made consistent within the nonlinear variational minimization. Let us finally mention that these sensitivities can obviously be computed with the adjoint model if it is available.

The iterative minimization is stopped when  $\|\mathbf{w}^{(j)} - \mathbf{w}^{(j-1)}\|$  reaches a predetermined threshold,  $e$ . Let us denote by  $\mathbf{w}_0^*$  the solution of the cost function minimization. The  $\star$  symbol will be used with any quantity obtained at the minimum. Subsequently, a posterior ensemble can be generated at  $t_0$  by

$$\mathbf{E}_0^* = \mathbf{x}_0^* \mathbf{1}^T + \sqrt{m-1} \mathbf{X}_0 \mathbf{W} \mathbf{U},$$

where

$$\mathbf{W} = \left[ \mathbf{I}_m + \sum_{k=L-S+1}^L (\mathbf{Y}_k^*)^T \mathbf{R}_k^{-1} \mathbf{Y}_k^* \right]^{-\frac{1}{2}}, \quad (7.13)$$

$\mathbf{U}$  is an arbitrary orthogonal matrix that satisfies  $\mathbf{U} \mathbf{1} = \mathbf{1}$  meant to keep the posterior ensemble centered on the analysis, and  $\mathbf{x}_0^* = \bar{\mathbf{x}}_0 + \mathbf{X}_0 \mathbf{w}_0^*$ . The update of the anomalies,  $\mathbf{X}_0^* = \mathbf{X}_0 \mathbf{W}$ , is a right transform of the initial anomalies,  $\mathbf{X}_0$ . A left transform more suitable for hybrid IEnKS and covariance localization could be used instead [Bocquet, 2016]. If filtering is considered, it additionally requires an independent model forecast throughout the DAW and possibly beyond the present time for forecasting.



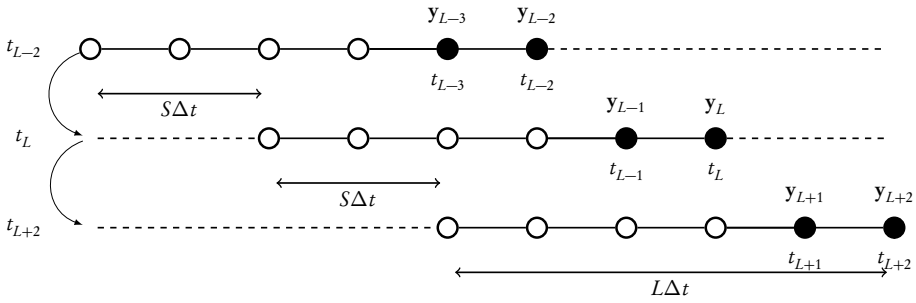


**Figure 7.2.** Cycling of the SDA IEnKS, where  $L = 5$  and  $S = 2$ , in units of  $\Delta t$ , the time interval between two updates. The method performs a smoothing update throughout the window but only assimilates the newest observation vectors (that have not been already assimilated), marked by black dots. Note that the time index of the dates and the observations is absolute for this schematic, not relative.

#### 7.4.1.2 ■ Forecast step

During the forecast step of the scheme cycle, the ensemble is propagated for  $S\Delta t$ , with  $S$  an integer introduced via (7.10):

$$\mathbf{E}_S^* = \mathcal{M}_{S;0}(\mathbf{E}_0^*).$$

This forecast ensemble at  $t_S$  will form the prior for the next analysis. A typical cycling of the analysis and forecast steps is schematically displayed in Figure 7.2.

A pseudocode of the IEnKS is proposed in Algorithm 7.1. It describes a full cycle of the (single data assimilation or SDA) IEnKS that includes the analysis and forecast steps, with the exception of the model forecast within the DAW required to complete the analysis for all times in the DAW, which is independent from the main IEnKS cycle.

Because it combines the propagation of the errors via the ensemble with a non-linear 4D variational analysis, the IEnKS has been shown to outperform 4D-Var, the EnKF, and the EnKS on several low-order models (Lorenz-63, Lorenz-95, Lorenz-95 coupled to a tracer model or a chemistry model, and a 2D barotropic model). This good performance persisted in all tested regimes of nonlinearity, applied to smoothing, filtering, or forecasting. It was also shown to be useful for parameter estimation because it combines the straightforward state augmentation technique of the EnKF with a variational analysis where the adjoint sensitivity to the parameters is estimated within the scheme in ensemble subspace [Bocquet and Sakov, 2013; Haussaire and Bocquet, 2016]. The only fundamental approximations of the IEnKS scheme are the Gaussian assumption made in the generation of the posterior ensemble and the second-order statistics assumption made when estimating the prior from the ensemble. When  $S = L$ , and using only the first iteration of the minimization, the single DA transform variant IEnKS then becomes formally equivalent to the so-called 4D-ETKF [Hunt et al., 2004]. As such, it can also be understood as a rigorously derived generalization of the 4D-EnVar methods. In the case where  $S = 1$  and  $L = 0$ , it also coincides with an ensemble-transform variant of the MLEF [Zupanski, 2005].

The performance of the single DA IEnKS has been compared to that of 4D-Var and the EnKF/EnKS with the Lorenz-95 model as a function of the DAW length. The results are shown in Figure 7.3. This follows up on the initial illustration of this chapter that compared 4D-Var with the EnKF. The shift,  $S$ , is chosen to be 1, which makes the

**Algorithm 7.1** A cycle of the lag- $L$ /shift- $S$ /SDA/bundle/Gauss-Newton IEnKS.

**Require:**  $t_L$  is present time. Transition model  $\mathcal{M}_{k+1;k}$ , observation operators  $\mathcal{H}_k$  at  $t_k$ . Algorithm parameters:  $\varepsilon, e, j_{\max}$ ,  $\mathbf{E}_0$ , the ensemble at  $t_0$ ,  $\mathbf{y}_k$  the observation at  $t_k$ .  $\mathbf{U}$  is an orthogonal matrix in  $\mathbb{R}^{m \times m}$  satisfying  $\mathbf{U}\mathbf{1} = \mathbf{1}$ .

- 1:  $j = 0, \mathbf{w} = \mathbf{0}, P = L - S + 1$
- 2:  $\mathbf{x}_0^{(0)} = \mathbf{E}_0 \mathbf{1} / m$
- 3:  $\mathbf{X}_0 = (\mathbf{E}_0 - \mathbf{x}_0^{(0)} \mathbf{1}^T) / \sqrt{m-1}$
- 4: **repeat**
- 5:    $\mathbf{x}_0 = \mathbf{x}_0^{(0)} + \mathbf{X}_0 \mathbf{w}$
- 6:    $\mathbf{E}_0 = \mathbf{x}_0 \mathbf{1}^T + \varepsilon \mathbf{X}_0$
- 7:    $\mathbf{E}_P = \mathcal{M}_{P;0}(\mathbf{E}_0)$
- 8:    $\bar{\mathbf{y}}_P = \mathcal{H}_P(\mathbf{E}_P) \mathbf{1} / m$
- 9:    $\mathbf{Y}_P = (\mathcal{H}_P(\mathbf{E}_P) - \bar{\mathbf{y}}_P \mathbf{1}^T) / \varepsilon$
- 10:   **for**  $k = P + 1, \dots, L$  **do**
- 11:      $\mathbf{E}_k = \mathcal{M}_{k;k-1}(\mathbf{E}_{k-1})$
- 12:      $\bar{\mathbf{y}}_k = \mathcal{H}_k(\mathbf{E}_k) \mathbf{1} / m$
- 13:      $\mathbf{Y}_k = (\mathcal{H}_k(\mathbf{E}_k) - \bar{\mathbf{y}}_k \mathbf{1}^T) / \varepsilon$
- 14:   **end for**
- 15:    $\nabla \mathcal{J} = \mathbf{w} - \sum_{k=P}^L \mathbf{Y}_k^T \mathbf{R}_k^{-1} (\mathbf{y}_k - \bar{\mathbf{y}}_k)$
- 16:    $\mathbf{H} = \mathbf{I}_m + \sum_{k=P}^L \mathbf{Y}_k^T \mathbf{R}_k^{-1} \mathbf{Y}_k$
- 17:   Solve  $\mathbf{H} \Delta \mathbf{w} = \nabla \mathcal{J}$
- 18:    $\mathbf{w} := \mathbf{w} - \Delta \mathbf{w}$
- 19:    $j := j + 1$
- 20: **until**  $\|\Delta \mathbf{w}\| \leq e$  **or**  $j \geq j_{\max}$
- 21:  $\mathbf{E}_0 = \mathbf{x}_0 \mathbf{1}^T + \sqrt{m-1} \mathbf{X}_0 \mathbf{H}^{-\frac{1}{2}} \mathbf{U}$
- 22:  $\mathbf{E}_S = \mathcal{M}_{S;0}(\mathbf{E}_0)$

system close to *quasi-static*: for large  $L$  the DAW is slightly shifted at each iteration. We can expect that the underlying cost function is only slightly modified from one analysis to the next, so that the global minimum can more easily be tracked (following the ideas initially developed by Pires et al. [1996]). The SDA IEnKS performs as theoretically expected up to  $L = 15$  for filtering and up to  $L = 30$  for smoothing. Beyond these lengths the performance deteriorates. In the regime where the IEnKS is reliable, it clearly outperforms 4D-Var and the EnKS. Again, this performance is due to (i) the flow dependence of the error, (ii) the fully nonlinear analysis within the DAW, and, to a lesser extent, (iii) the quasi-static  $S = 1$ .

### 7.4.2 ■ Single and multiple assimilation of observations

An important idea of the IEnKS is to assimilate observations far ahead in time from the updated state at  $t_0$ . This is meant to stabilize the scheme in the directions of the unstable modes of the chaotic model. This has been shown to be very efficient but ultimately fails for DAWs that are too long. An idea to stabilize the system for long DAWs is to assimilate more observations within the DAW. Depending on the precise choice of  $S$  and  $L$ , this may lead to assimilating observations several times, which is statistically inconsistent. Let us see how such a design can actually be justified [Bocquet and Sakov, 2014].

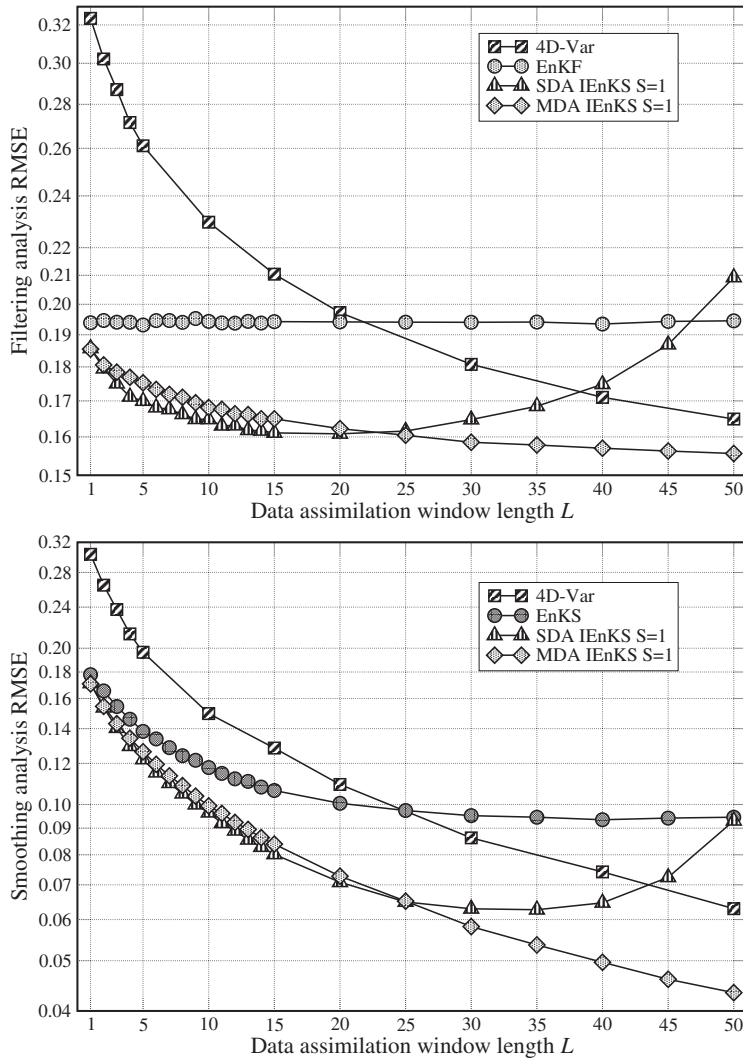


**Figure 7.3.** Synthetic data assimilation experiments with the Lorenz-95 model, which show the theoretical superiority of the IEnKS regardless of its numerical cost. The upper panel shows the filtering analysis RMSE of optimally tuned EnKF, 4D-Var, IEnKS assimilation experiments, as a function of the length of the DAW. The lower panel shows the smoothing analysis RMSE of optimally tuned EnKS, 4D-Var, and IEnKS as a function of the length of their DAW. The optimal RMSE is chosen within the window for 4D-Var and it is taken at the beginning of the window for the IEnKS. The EnKF, EnKS, and IEnKS use an ensemble of  $m = 20$  which avoids the need for localization but requires inflation. The length of the DAW is  $L \times \Delta t$ , where  $\Delta t = 0.05$ . Both RMSEs for the SDA and MDA IEnKS are shown.

The IEnKS cost function can be generalized with the goal of assimilating any observation within the DAW,

$$\mathcal{J}(\mathbf{w}) = \sum_{k=0}^L \frac{\beta_k}{2} \|\mathbf{y}_k - \mathcal{F}_{k:0}(\bar{\mathbf{x}}_0 + \mathbf{X}_0 \mathbf{w})\|_{\mathbf{R}_k}^2 + \frac{1}{2} \|\mathbf{w}\|^2, \quad (7.14)$$

which introduces a set of coefficients,  $0 \leq \beta_k \leq 1$ , that weight the innovation terms.

There are some degrees of freedom in the choice of  $L$ ,  $S$ , and the  $\{\beta_k\}_{0 \leq k \leq L}$ . Let us just mention a few legitimate choices for them. First, for any choice of  $L$  and  $S$  such that  $1 \leq S \leq L+1$ , the most natural choice for the  $\{\beta_k\}_{0 \leq k \leq L}$  is to set  $\beta_k = 1$  for  $k = L-S+1, \dots, L$ , and  $\beta_k = 0$  otherwise. That way, the observations are assimilated once and only once. This leads back to the original formulation of the IEnKS (7.10) and explains why it was called the single data assimilation scheme (SDA IEnKS). It is simple, and the optional analysis of the update step is merely a forecast of the analyzed state at  $t_0$ , or possibly a forecast of the full ensemble from  $t_0$ . When  $S \geq L$ , the DAWs do not overlap, while they do so if  $S < L$ .

For very long DAWs, the use of *multiple data assimilation* (or *splitting*) of observations, denoted MDA in the following, can be proven to be numerically efficient. An observation vector  $\mathbf{y}$  is said to be assimilated with weight  $\beta$  ( $0 \leq \beta \leq 1$ ) if the following Gaussian observation likelihood is used in the analysis:

$$p(\mathbf{y}^\beta | \mathbf{x}) = \frac{e^{-\frac{\beta}{2} \|\mathbf{y} - \mathcal{H}(\mathbf{x})\|_{\mathbf{R}}^2}}{\sqrt{(2\pi/\beta)^p |\mathbf{R}|}}, \quad (7.15)$$

where  $|\mathbf{R}|$  is the determinant of  $\mathbf{R}$ . The upper index of  $\mathbf{y}^\beta$  refers to its partial assimilation with weight  $\beta$ . The prior errors attached to the several occurrences of one observation are *chosen* to be independent. In that light, the  $\{\beta_k\}_{0 \leq k \leq L}$  are merely the weights of the observation vectors  $\{\mathbf{y}_k\}_{0 \leq k \leq L}$  within the DAW. Statistical consistency imposes that a unique observation vector be assimilated so that the sum of all its weights in the DA experiment is one. For instance, if  $1 = S \leq L+1$ , one requires  $\sum_{k=0}^L \beta_k = 1$ . In the more general case where the observation vectors have the same number of nonzero weights, then  $L$  is a multiple of  $S$ :  $L = QS$ , where  $Q$  is an integer. As a result, consistency requires  $\sum_{q=0}^{Q-1} \beta_{Sq+l} = 1$ , with  $l = 0, \dots, S$ .

In the MDA case, unlike the SDA subcase, the optional estimation of the  $\mathbf{x}_k$  states, besides  $\mathbf{x}_0$ , within the DAW is more complex. It requires reweighting the observations within the DAW and performing a second analysis within the DAW with these balanced weights. More details can be found in Bocquet and Sakov [2014] about this so-called balancing step.

Note that when the constraint  $\sum_{k=0}^L \beta_k = 1$  is not satisfied, the underlying smoothing PDF will not be the targeted one but, with well-chosen  $\{\beta_k\}_{0 \leq k \leq L}$ , could be a power of it, which can be put to use.

The chaining of the DA cycles in the MDA case is displayed in Figure 7.4. A pseudocode of the MDA IEnKS is proposed in Algorithm 7.2. It describes a full cycle of the (MDA) IEnKS that includes the analysis at the beginning of the DAW and the forecast step, with the exception of the balancing step, which is required to complete the analysis for all times in the DAW, but which is independent from the main IEnKS cycle.

These MDA approaches are mathematically consistent in the sense that they are demonstrated to be correct in the linear model Gaussian statistics case. In Bocquet and Sakov [2014], a heuristic argument based on Bayesian ideas justifies the use of the method in the nonlinear case.

The accuracy of the SDA and MDA IEnKS, as well as 4D-Var and the EnKF, is compared in Figure 7.3. The results emphasize the accuracy of the IEnKS compared to 4D-Var and the EnKF. Moreover, the SDA IEnKS is shown to be more accurate than the MDA IEnKS for short DAWs, since the latter is not as consistent with nonlinear models. Yet, the MDA IEnKS is much more stable for longer DAWs.

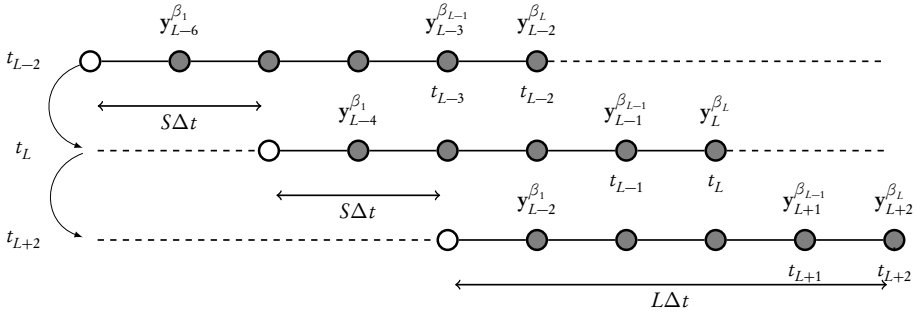


**Figure 7.4.** Chaining of the MDA IEnKS cycles. The schematic illustrates the case  $L = 5$  and  $S = 2$ . The method performs a smoothing update throughout the window, potentially using all observations within the window (marked by gray dots), except for the first observation vector, assumed to be already entirely assimilated. Note that the time index for the dates and the observations is absolute for this schematic, not relative.

---

**Algorithm 7.2** A cycle of the lag- $L$ /shift- $S$ /MDA/bundle/Gauss-Newton IEnKS.

---

**Require:**  $t_L$  is present time. Transition model  $\mathcal{M}_{k+1:k}$ , observation operators  $\mathcal{H}_k$  at  $t_k$ . Algorithm parameters:  $\varepsilon$ ,  $e$ ,  $j_{\max}$ ,  $\mathbf{E}_0$ , the ensemble at  $t_0$ ,  $\mathbf{y}_k$  the observation at  $t_k$ .  $\mathbf{U}$  is an orthogonal matrix in  $\mathbb{R}^{m \times m}$  satisfying  $\mathbf{U}\mathbf{1} = \mathbf{1}$ .  $\beta_k$  for  $k = 0, \dots, L$  are the weights (see main text).

- 1:  $j = 0$ ,  $\mathbf{w} = \mathbf{0}$
  - 2:  $\mathbf{x}_0^{(0)} = \mathbf{E}_0 \mathbf{1} / m$
  - 3:  $\mathbf{X}_0 = (\mathbf{E}_0 - \mathbf{x}_0^{(0)} \mathbf{1}^T) / \sqrt{m-1}$
  - 4: **repeat**
  - 5:    $\mathbf{x}_0 = \mathbf{x}_0^{(0)} + \mathbf{X}_0 \mathbf{w}$
  - 6:    $\mathbf{E}_0 = \mathbf{x}_0 \mathbf{1}^T + \varepsilon \mathbf{X}_0$
  - 7:    $\bar{\mathbf{y}}_0 = \mathcal{H}_0(\mathbf{E}_0) \mathbf{1} / m$
  - 8:    $\mathbf{Y}_0 = (\mathcal{H}_0(\mathbf{E}_0) - \bar{\mathbf{y}}_0 \mathbf{1}^T) / \varepsilon$
  - 9:   **for**  $k = 1, \dots, L$  **do**
  - 10:      $\mathbf{E}_k = \mathcal{M}_{k:k-1}(\mathbf{E}_{k-1})$
  - 11:      $\bar{\mathbf{y}}_k = \mathcal{H}_k(\mathbf{E}_k) \mathbf{1} / m$
  - 12:      $\mathbf{Y}_k = (\mathcal{H}_k(\mathbf{E}_k) - \bar{\mathbf{y}}_k \mathbf{1}^T) / \varepsilon$
  - 13:   **end for**
  - 14:    $\nabla \mathcal{J} = \mathbf{w} - \sum_{k=0}^L \beta_k \mathbf{Y}_k^T \mathbf{R}_k^{-1} (\mathbf{y}_k - \bar{\mathbf{y}}_k)$
  - 15:    $\mathbf{H} = \mathbf{I}_m + \sum_{k=0}^L \beta_k \mathbf{Y}_k^T \mathbf{R}_k^{-1} \mathbf{Y}_k$
  - 16:   Solve  $\mathbf{H} \Delta \mathbf{w} = \nabla \mathcal{J}$
  - 17:    $\mathbf{w} := \mathbf{w} - \Delta \mathbf{w}$
  - 18:    $j := j + 1$
  - 19: **until**  $\|\Delta \mathbf{w}\| \leq e$  **or**  $j \geq j_{\max}$
  - 20:  $\mathbf{E}_0 = \mathbf{x}_0 \mathbf{1}^T + \sqrt{m-1} \mathbf{X}_0 \mathbf{H}^{-\frac{1}{2}} \mathbf{U}$
  - 21:  $\mathbf{E}_S = \mathcal{M}_{S:0}(\mathbf{E}_0)$
-

Greater stability can be achieved with the SDA IEnKS when using a quasi-static variational assimilation within each analysis, a procedure that may have a significant numerical cost depending on the implementation (A. Fillion, M. Bocquet, and S. Gratton, personal communication).

### 7.4.3 ■ Localization

Like any EnVar approach, the IEnKS requires localization for a suitable use with high-dimensional models. Localization of the IEnKS is as difficult as with 4DVar. It can be even more critical, since localization may partially destroy the consistency between consecutive iterations in the nonlinear variational analysis. As for 4DVar, an approximate solution consists of propagating the ensemble within the DAW, but also the localization operator using a surrogate advection model. This also enables the estimation of the updated ensemble. However, if an adjoint of the model is available, it becomes possible, as in En-4DVar or 4D-Var-Ben, to exactly (albeit implicitly) propagate localization within the DAW. Going further than En-4DVar or 4D-Var-Ben, the adjoint also enables an exact construction of the updated ensemble. More details on the theory and numerical results are given in Bocquet [2016].

Figure 7.5 shows an example of the IEnKS with the Lorenz-95 model used in conjunction with localization. The ensemble is set to  $m = 10$ , lower than the dimension of the unstable and neutral subspace of the model (14), which means that localization is mandatory. It appears from this experiment that, at least in this idealized context, a covariant (i.e., evolving with the model flow) localization achieves a performance as good as that of an IEnKS with localization where the model adjoint is available and where the localized covariances are implicitly propagated.

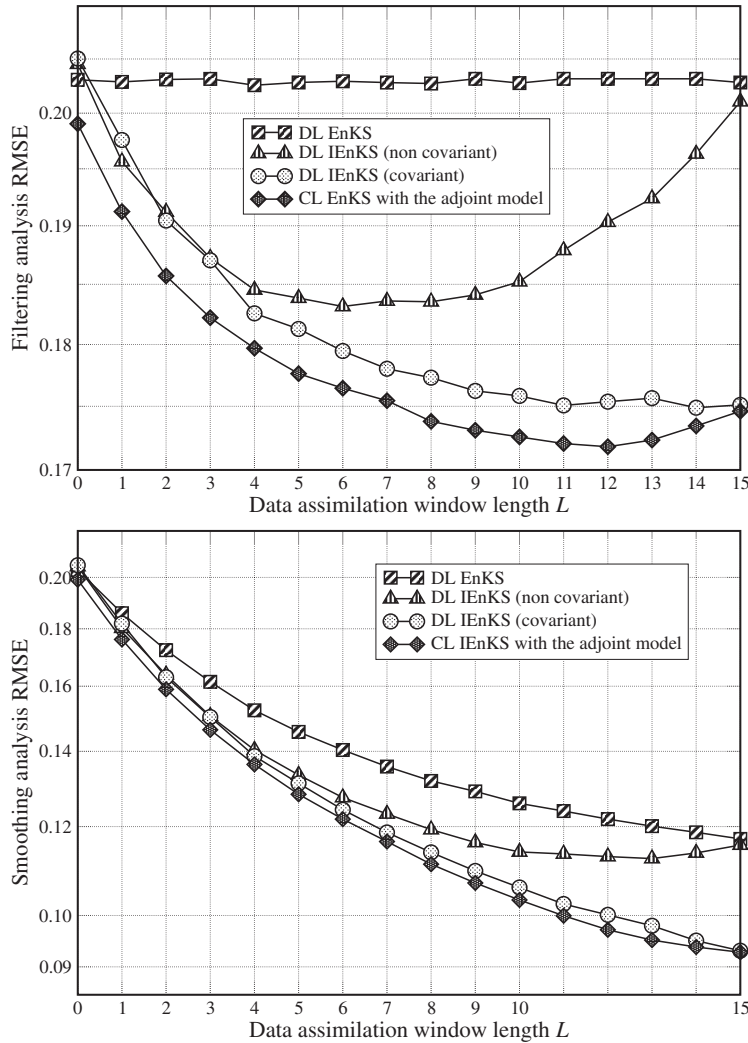


**Figure 7.5.** Synthetic DA experiments with the Lorenz-95 model to compare several localization strategies when  $m = 10$ . The inflation is optimally tuned. The upper panel shows the filtering analysis RMSE as a function of the length of the DAW. The lower panel shows the smoothing analysis RMSE as a function of the length of the DAW. Four local methods are compared: a DL (domain localization) EnKF/EnKS, the IEnKS with a static domain (i.e., noncovariant) localization, the IEnKS where the local domains are covariantly advected eastward with the velocity  $v = 6$  grid cells per time unit, and a flow-dependent covariance localization IEnKS where the adjoint is supposed to be available and used. Covariance localization and domain localization use a Gaspari–Cohn localization function of radius 12 grid cells (see Section 6.5). The length of the DAW is  $L \times \Delta t$ , where  $\Delta t = 0.05$ . Adapted from Bocquet [2016].